

NASA Technical Memorandum 104486

1N-20

21400

β.8

Full-Size Solar Dynamic Heat Receiver Thermal-Vacuum Tests

(NASA-TM-104486) FULL-SIZE SOLAR DYNAMIC
HEAT RECEIVER THERMAL-VACUUM TESTS (NASA)
CSCL 108

N91-25164

Uncles
63/20 0021400

L.M. Sedgwick and K.J. Kaufmann
Boeing Aerospace and Electronics
Seattle, Washington

and

K.L. McLallin and T.W. Kerslake
Lewis Research Center
Cleveland, Ohio

Prepared for the
26th Intersociety Energy Conversion Engineering Conference
cosponsored by ANS, SAE, ACS, AIAA, ASME, IEEE, and AIChE
Boston, Massachusetts, August 4-9, 1991

NASA

FULL-SIZE SOLAR DYNAMIC HEAT RECEIVER THERMAL-VACUUM TESTS

L.M. Sedgwick and K.J. Kaufmann
Boeing Aerospace and Electronics
Seattle, Washington

K.L. McLallin and T.W. Kerslake
National Aeronautics and Space Administration
Lewis Research Center
Cleveland, Ohio

ABSTRACT

The first ever testing of a full-size, 102 kWt, solar dynamic heat receiver utilizing high-temperature thermal energy storage has been completed. The purpose of the test program was to quantify receiver thermodynamic performance, operating temperatures, and thermal response to changes in environmental and power module interface boundary conditions. The heat receiver was tested in a vacuum chamber with liquid nitrogen cold shrouds and an aperture cold plate to partially simulate a low-Earth-orbit environment. The cavity of the receiver was heated by an infrared quartz lamp heater with 30 independently controllable zones to allow axially and circumferentially varied flux distributions. A closed-Brayton cycle engine simulator conditioned a helium-xenon gas mixture to specific interface conditions to simulate the various operational modes of the solar dynamic power module on the Space Station Freedom. Inlet gas temperature, pressure, and flow rate were independently varied. A total of 58 simulated orbital cycles, each 94 minutes in duration, was completed during the test conduct period.

INTRODUCTION

A full-size, 102 kWt, solar dynamic heat receiver utilizing high-temperature thermal energy storage was tested to quantify the receiver thermodynamic performance and its thermal response to changes in environmental and power module interface boundary conditions. The test program was conducted for the NASA Lewis Research Center [1]. The heat receiver was tested in a vacuum chamber with liquid nitrogen (LN₂) cold shrouds and cold plate to partially simulate a low-Earth-orbit environment. The testing was conducted by Boeing Aerospace & Electronics (BA&E) during the period 9 October through 3 November 1990 at the Tulalip Hazardous Test Site, located in Marysville, WA.

The heat receiver was designed to meet the requirements specified for the solar

dynamic power modules on the Space Station Freedom [2]. The 25 kW of electrical power supplied to the user requires a nominal 102 kW of thermal power delivered to the closed-Brayton cycle (CBC) heat engine throughout a 94 minute orbit, including when the space craft is eclipsed for up to 36 minutes from the sun. The receiver employs an integral thermal energy storage system that utilizes the latent heat available through phase change of a eutectic salt mixture of lithium fluoride and calcium difluoride. The salt mixture has a melt temperature of about 1420°F. The salt is contained within a nickel felt matrix used to enhance heat transfer and to control the locations of voids that form during solidification. The heat receiver was designed and fabricated for NASA by BA&E [3,4,5].

Special test equipment was designed and fabricated including a 250 kW quartz lamp heater that mounts inside the receiver cavity to supply the simulated sun energy and a CBC engine simulator that circulates the gas through the receiver, removes heat, and conditions the gas to achieve the inlet temperatures, pressures, and flow rates required to simulate various power cycle operating modes.

The receiver was tested inside a vacuum chamber to preclude convection effects and installed in a horizontal orientation to minimize the influence of gravity on the salt void distribution in the felt metal material [4,5]. Temperatures, pressures, heater power, and gas flow rate were recorded during the test conduct. Heater power, heater duty cycle, inlet gas temperature, gas pressure, and gas flow rate were independently varied. An optical borescope was used throughout the test to observe and photograph the receiver cavity.

This paper describes the test conduct and provides summaries of some of the test data. Descriptions of the test hardware, facilities, and instrumentation are described in a companion paper [6]. A more detailed discussion of the test data

and its correlation with thermal analyses will be the subject of a future publication. Post test inspections of the test article and support hardware are described in the test report [7].

TEST CONDUCT

Steady-State Heat Balance Tests

The steady-state heat balance tests provided (1) a slow and controlled heat up to allow insulation and other materials to off-gas during the initial heat up of the receiver; (2) a condition for maintaining high receiver temperatures without operation of the CBC engine simulator; (3) a slow and controlled initial melting of the salt; and (4) heat loss data for thermal model correlation. The quartz lamps were operated at low voltage to reduce the risk of corona during the potentially high off-gassing periods.

Test mode VT.1 was completed when the receiver cavity had maintained stabilized temperatures near 1000°F. The total time to achieve this condition after activating the heater zones was about 43 hours and approximately 6.8 kW of electrical power was required to maintain this temperature in the cavity. No significant events occurred during this test mode.

Test mode VT.2 continued the controlled heat up of the receiver cavity to 1600°F. The initial heat up to the salt melt temperature, thermal arrest of the salt in the heat storage tubes, and continued heat up to a cavity temperature of about 1540°F occurred without any significant anomalies. During thermal arrest, the heater zones were powered at 26 kW to achieve a complete melt of the salt over a period of about 6 hours.

The first of 3, long-term out-gassing periods began during test mode VT.2, about 60 hours after initiation of testing. This event lasted approximately 7 hours and the chamber pressure rose from 5×10^{-6} torr to about 1.5×10^{-4} torr. Shut down of the heater was not required. Shortly after the vacuum event ended, electrical power was lost to facility systems except for the vacuum equipment. The cavity was at a temperature of about 1550°F. The power problem required about 3 hours to repair. A loss of shroud and cold plate LN₂ flow during the first few minutes of the power outage resulted in several problems, the most obvious being a rapid increase in chamber pressure to the 10^{-3} torr range. This was caused by the sudden increase in cold plate temperature from -240°F to about 100°F which volatilized off-gassing materials that had collected

onto its surface. Some of the liberated material condensed onto the actively cooled front lens of the borescope causing optical distortions of viewed objects throughout the remainder of testing. The rapid increase in temperature also caused tape adhesive that held 2 thermocouples onto the cold plate surface to de-bond and fall off. These were the only transducers lost during the conduct of testing.

A second major off-gassing event occurred after power was restored and cavity temperatures were approaching 1600°F. This event required a manual shut down of the heaters. The chamber vacuum level was initially at 4×10^{-6} torr and degraded to the 10^{-2} torr level. The CBC simulator was quickly filled with argon gas and operated to freeze the salt inside the heat storage tubes. Heater operation was then resumed at low power. After about 7 hours, the chamber vacuum level began to increase rapidly and finally stabilized at 2×10^{-6} torr. Test mode VT.2 was terminated with the cavity temperatures at about 1300°F after 125 hours of elevated temperature exposure.

Verification Tests

The heat receiver was designed to continuously deliver 102 kWt to a mixture of helium and xenon gas (molecular weight of 40) with 198 kW of solar power input to the cavity for 58 minutes of a 94 minute orbit. Baseline engine interface parametric values used to design the receiver include a gas inlet temperature of 900°F, an inlet pressure of 92 psia, and a mass flow rate of 117 lbm/min.

Test mode VT.3 operated the receiver using the baseline conditions listed above and was repeated several times to quantify any changes over the test period. The distribution of electrical power input to the 30 quartz lamp heater zones simulated that from an on-axis, parabolic concentrator [5]. Each of the circumferential zones (6 at each of 5 axial locations) operated at nearly the same power level. The percentage of total heater power distributed to each of the 5 axial zones from the front (aperture) to rear (back wall) of the cavity varied as follows: 33%, 32%, 15%, 11%, and 9%.

Test mode VT.3 was initiated with a full power sunlit period. The cavity was at a temperature of about 1300°F and the heat storage tubes were fully discharged (salt frozen). The CBC engine simulator was charged with 35 psig of premixed, bottled, helium-xenon gas and the blower was activated. The 30 heater zones were then slowly ramped to full power, 1 zone at a

time, beginning at the rear of the cavity (lowest power) and working forward. Additional helium-xenon gas was introduced into the CBC piping at several different times during the first several orbits to increase the inlet static pressure. Reasonably stabilized temperatures were achieved by the 8th orbital simulation and test mode VT.3 was terminated.

Test mode VT.5 was the first of 2 gradual transitions to begin the simulation of a maximum insolation, perihelion orbit by changing only one variable at a time. Test mode VT.5 was initiated at the beginning of the 9th orbit by increasing the gas flow rate from 117 lbm/min to 165 lbm/min. All other interfaces were maintained at the baseline settings.

During test mode VT.3, chamber vacuum cycled within the 10^{-6} torr range as cavity temperatures varied through the orbital cycles. This behavior suddenly changed during the 9th orbit when the final and longest-term out-gassing event began. Chamber pressure rose steadily up to the 10^{-4} torr range and was no longer influenced by changes in cavity temperature. Test mode VT.5 was terminated with marginal temperature stabilization at the end of the 12th orbital simulation because of an increased risk of corona at the higher pressure levels.

During the next 13 hours, the CBC engine simulator was shut off and the heater zones were operated at about 18 kW to maintain cavity temperatures just below the melt temperature of the salt. It is worth noting that lowering the cavity temperatures below the salt melt temperature during all 3 out-gassing events had no effect on the chamber vacuum level. It is reasonable to assume, therefore, off-gassing sources were external to the receiver cavity. The chamber vacuum level continued to fluctuate until it began to stabilize in the low 10^{-4} torr range and the decision was made to continue with testing despite the higher pressure level to preserve test dollars.

Orbital variation test mode VT.6 changed the heater duty cycle to simulate a 66 minute sun period in a 94 minute perihelion orbit. Continued high-temperature cycling inside the cavity did not influence vacuum chamber pressure level and no significant events occurred during the conduct of test mode VT.6. This test condition was terminated at the end of the 17th orbital simulation after temperature stabilization had been achieved.

Test mode VT.8 simulated maximum insolation orbits and was initiated by increasing the total power to the quartz lamp heater from 198 kW to 224 kW. The percentage of the total power distributed per heater zone matched the baseline. Gas inlet temperature was increased slightly to 915°F.

A number of heater problems were encountered during the conduct of this test mode and it was not clear if they were related to problems in the quartz lamp power controllers or whether they could be attributed to corona inside the receiver cavity. Test mode VT.8 was declared complete at the end of the 21st orbital simulation, prior to achieving complete stabilization of temperatures because of corona concerns.

An attempt was made to simulate peaking orbits during test mode VT.12 but the CBC simulator could not provide the low flow rate required (the receiver pressure drop was lower than pretest predictions). As a result, 5 orbits were simulated at near-baseline conditions. During these orbits, the major vacuum off-gassing event that had begun almost 25 hours before the initiation of this test mode finally ended and chamber vacuum returned to the 10^{-5} torr range. Vacuum level began to once again cycle with cavity temperatures. Cavity temperatures stabilized by the end of the 26th orbital simulation and the test mode was terminated.

Flux Variation Tests

Test mode SS.1 was initiated with the sunlit period of the 27th orbit and was conducted to examine the change in receiver performance and operating temperatures with an axially modified distribution of heater power. The distribution was obtained by averaging circumferential flux values predicted for the off-axis concentrator design for Freedoms solar dynamic power module [8]. The peak flux was moved forward in the cavity because of the shorter heat storage tube length in this heat receiver concept. All other interfaces were maintained at the baseline values. No significant events occurred and test mode SS.1 was terminated with stabilized temperatures at the end of the 34th orbital simulation. Chamber vacuum levels continued to improve, returning to the 10^{-6} torr level and cycled with cavity temperatures.

Test mode SS.4 was conducted to quantify the change in receiver performance and operating temperatures with a non-uniform circumferential flux distribution. Baseline interface parameters were

maintained during the test mode. No unplanned events occurred and normal vacuum levels continued and cycled with cavity temperatures. Test mode SS.4 was terminated with stabilized temperatures at the end of the 37th orbital simulation.

The flux variation tests were concluded with a return to the baseline orbital conditions. First, however, a slightly modified baseline test mode (VT.3B) was conducted beginning with the sunlit period of the 38th orbit by increasing the total quartz lamp heater power by 7 kW to 205 kW. The percentage of the total power distributed between zones matched the baseline distribution and all other parameters were held constant at the baseline values. Normal vacuum levels continued and stabilized cavity temperatures were achieved by orbit #43. Heater power was then lowered back to 198 KW and 7 more orbits were simulated at baseline conditions (test mode VT.3A) in preparation for a shut down to ambient temperature. Normal vacuum levels continued, stabilized temperatures were achieved, and test mode VT.3A was terminated at the conclusion of the 50th simulated orbit.

Cold Soak Shut Down and Start Up

Shut down to ambient was begun after the 36 minute eclipse period of orbit #50. The CBC engine simulator remained running with a mass flow rate of 117 lbm/min until the gas temperature exiting the receiver dropped below 1000°F. The blower bypass valve was then completely shut off forcing full flow through the receiver and the regenerator bypass valves were fully opened to obtain the coolest possible inlet gas temperature. The CBC was operated in this condition until the difference between the inlet and exit gas temperatures dropped below 2°F. Additional cooling was then provided only by the LN₂ aperture cold plate and cold shrouds.

Test mode CS.3 was run to simulate the rapid start up of the heat receiver from a cold soak condition. The test mode was begun with the heat storage tubes at a temperature of about 90°F and chamber vacuum at 7×10^{-7} torr. The 30 quartz lamp zones were powered up at the baseline power levels and no gas was circulated through the receiver during the first complete orbital simulation (#51). Gas flow was initiated approximately 15 minutes into the second heat up period and baseline interface conditions were obtained over the next few orbits. The first two orbital periods proceeded without any significant problems.

However, during 53rd orbit, heater zones began to show signs of corona although the vacuum chamber pressure did not show any significant degradation. Finally, after the 58th orbital simulation, the test conductor terminated testing because electrical power to many of the heater zones could not be sustained. The receiver and vacuum facilities were slowly brought back to ambient conditions over a 2 day period. Results of post-test inspections are given in Reference [7].

RESULTS

Plots of receiver temperatures and interface parameters as a function of time are not included in this paper due to space limitations but are provided in reference [7]. However, several tables of data are provided to summarize receiver performance parameters and receiver operating temperatures during the various test modes executed. The data shown in these summaries were obtained from the most stabilized orbits (or period) for each of the test modes executed.

Receiver Thermodynamic Performance

A summary of the thermodynamic and performance parameters by test mode is given in Figure 1. Values shown for the quartz lamp power were averaged over the sunlit period. The ambient temperatures, gas flow rates, static pressures, and values of pressure drop across the receiver were averaged over the entire orbital period including eclipse.

Values of receiver efficiency shown in Figure 1 were integrated over the entire orbit and are dependant on the degree of stabilization achieved during the test mode. Less stabilized conditions show lower or higher efficiencies because more energy is stored or recovered as sensible heat during the transient period between test modes. Efficiencies for the more stabilized orbits using baseline or near baseline parameters show an integrated receiver thermal efficiency of about 84 percent and relatively little variation is seen between stabilized receiver operating modes.

Pressure drop through the receiver is an important parameter for improving Brayton cycle efficiency. Measured pressure drops through the receiver were about 1% of the inlet static pressure at 92 psia. There was no indication of gas flow distribution problems between heat storage tubes.

Receiver Operating Temperatures

Figure 2 lists the maximum and minimum heat storage tube surface temperatures, internal salt temperatures, and cavity side-wall temperatures. The maximum surface temperatures for heat storage tubes 12 and 19 show that the flux level, rather than interface conditions (i.e., gas flow rate, inlet temperature, etc.), control the peak temperatures. All of the test modes that operated with a total heater power near the baseline value of 198 kW show peak surface temperatures on these 2 heat storage tubes of about 1680°F regardless of the other receiver boundary conditions. Test modes VT.8 (224 kW) and VT.3B (205 kW) produced peak temperatures greater than 1700°F. In contrast are the internal salt temperatures which show significant changes in temperature range with variations in the tube side boundary conditions. Thus, heat storage tube surface temperatures that face the quartz lamp heater have significant radiation errors. Surface temperatures shown for tube 4 were measured in the convection valleys and appear to be more accurate because of the increase in contact area between the thermocouple and the tube wall.

Cavity side-wall temperatures appear to be more accurate and are a better indicator of maximum cavity temperatures because the thermocouples were covered with a quartz cloth patch and had no direct view to the heater lamps. Cavity temperatures ranged from about 1300°F to 1650°F during baseline operating modes. Therefore, heat storage tube surface temperatures were likely limited to the same range.

The exiting gas temperature over the most stabilized orbits from each of the test modes are compared in Figure 3. The receiver design requirement of 1300°F±50°F was met for all of the test modes except for VT.5 and VT.6, neither of which simulates an actual design condition.

SUMMARY

The test program successfully demonstrated that a full-size solar dynamic heat receiver can be operated on Earth and in vacuum to quantify performance. The heat receiver met almost all of its design requirements during the simulation of Space Station Freedom operational modes. Thermodynamic performance compared with predictions although receiver losses through the cavity insulation were higher than expected. The high heat flux and poor contact between thermocouples and surfaces of the heat storage tubes introduced significant errors into these

measurements. However, comparison of these measurements with those made on the cavity walls show cavity temperatures remained below design limitations.

Comparison of the test mode data shows that receiver performance, maximum operating temperatures, and temperature gradients do not vary significantly between the power module operating modes simulated. The cavity radiation exchange appears to effectively smooth maldistributed incident flux although further analyses is required to estimate what incident flux profiles were actually produced from the off-design quartz lamp power distributions.

Additional tasks that may be completed at a later date include (1) correlation of test and thermal model data; (2) additional analyses of the felt metal/bellows/salt interactions; (3) detailed inspections of the heat storage tubes including computed tomography and sectioning; and (4) quantitative analyses of the off-gassing samples taken after test completion.

REFERENCES

- [1] NASA Contract NAS3-25716, "Advanced Development Receiver Testing in Thermal/Vacuum Environment", 1 Nov 1989, NASA Lewis Research Center, Cleveland, Ohio.
- [2] NASA Document LeRC-SS-003, "Solar Dynamic Power Module System Part I Contract End Item Specification", 3 Feb 1987, NASA Lewis Research Center, Cleveland, Ohio.
- [3] NASA Contract NAS3-24669, "Solar Dynamic Heat Receiver Technology", 1 Nov 1989, NASA Lewis Research Center, Cleveland, Ohio.
- [4] Sedgwick, L.M., "A Brayton Cycle Solar Dynamic Heat Receiver for Space", IECEC Proceedings, 1989.
- [5] Sedgwick, L.M., "Solar Dynamic Heat Receiver Technology - Final Report", NASA-CR-187040, Jan 1991.
- [6] Sedgwick, L.M., "Ground Test Program for a Full-Size Solar Dynamic Heat Receiver", IECEC Proceedings, 1991.
- [7] Sedgwick, L.M., "Advanced Development Heat Receiver Thermal/Vacuum Test With Cold Wall - Final Test Report", NASA-CR-187092, Jun 1991.
- [8] Jeffries, K.S., "Concentration of Off-Axis Radiation by Solar Concentrators for Space Power", IECEC Proceedings, 1989.

Test Mode	Avg Power	Avg Flow	Avg P	Avg ΔP	Avg T_{∞}	\dot{Q} Input	\dot{Q} Sun	\dot{Q} Ecl	\dot{Q} Loss	η
VT.1	6.8	0	0	-	47	-	-	-	-	-
VT.2	12.8	0	0	-	38	-	-	-	-	-
VT.3	193.5	117	89.5	1.0	52	183.9	92.8	60.2	30.9	83.2
VT.5	193.2	162	86.5	1.8	54	181.6	95.0	62.8	23.7	87.0
VT.6	197.0	166	91.0	1.8	49	213.5	126.4	55.9	31.2	85.4
VT.8	223.5	168	92.6	1.8	50	242.1	136.7	60.9	44.5	81.6
VT.12	197.9	117	94.0	0.9	48	188.1	95.1	61.4	31.5	83.2
SS.1	197.4	117	94.5	0.9	44	187.0	95.1	62.7	29.2	84.4
SS.4	196.3	117	94.8	0.9	50	186.5	95.8	61.1	29.6	84.1
VT.3B	204.9	117	95.4	1.0	40	194.5	99.4	63.4	31.6	83.7
VT.3A	198.0	117	94.8	1.1	37	191.4	98.3	64.2	29.0	84.9
CS.1	0	132	71.3	1.1	43	0	-	215.3	-	-
CS.3/1	197.7	0	53.8	0	41	190.7	0	0	190.7	0
CS.3/2	197.8	71	69.2	0.7	41	189.5	70.9	56.9	61.8	67.4
CS.3/4	195.0	113	91.7	1.1	44	182.3	83.1	56.2	43.1	76.4

Notes: Power = Lamp power in kW Flow = Gas flow rate in lbm/min
P = Inlet gas pressure in psia ΔP = Differential pressure in psid
 \dot{Q} = Total integrated energy in kW-hrs T_{∞} = Ambient temperature, °F

Figure 1: Measured Performance Parameters

Test Mode	TUBE #4		TUBE #12				TUBE #19				Cavity Walls			
	$T_{\text{max surf}}$	$T_{\text{min surf}}$	$T_{\text{max surf}}$	$T_{\text{min surf}}$	$T_{\text{max salt}}$	$T_{\text{min salt}}$	$T_{\text{max surf}}$	$T_{\text{min surf}}$	$T_{\text{max salt}}$	$T_{\text{min salt}}$	$T_{\text{max side}}$	$T_{\text{min side}}$	$T_{\text{max back}}$	$T_{\text{min back}}$
VT.1	1010	993	1019	989	1028	996	1020	994	1029	1002	1018	988	1010	996
VT.2	1514	1486	1528	1486	1539	1497	1529	1486	1540	1497	1523	1482	1575	1492
VT.3	1616	1314	1685	1292	1516	1229	1672	1375	1578	1396	1647	1305	1634	1358
VT.5	1626	1136	1672	1146	1431	1098	1656	1171	1449	1172	1621	1159	1603	1194
VT.6	1635	1294	1683	1264	1454	1192	1658	1365	1537	1383	1625	1290	1614	1330
VT.8	1658	1346	1710	1333	1488	1225	1697	1393	1599	1395	1672	1353	1653	1383
VT.12	1597	1333	1682	1296	1504	1233	1669	1382	1585	1397	1652	1316	1639	1372
SS.1	1595	1337	1683	1297	1480	1214	1673	1381	1578	1397	1652	1319	1633	1371
SS.4	1602	1333	1690	1298	1488	1219	1655	1380	1574	1395	1638	1320	1635	1372
VT.3B	1599	1383	1701	1329	1517	1236	1697	1391	1610	1402	1680	1352	1669	1384
VT.3A	1607	1333	1685	1288	1496	1217	1676	1373	1587	1397	1655	1309	1644	1367
CS.1	1350	90	1378	89	1374	89	1399	91	1422	90	1387	112	1372	120
CS.3/1	1575	87	1598	88	1428	88	1573	92	1415	88	1522	112	1488	116
CS.3/2	1597	1158	1659	1170	1428	1119	1639	1193	1449	1193	1601	1178	1589	1176
CS.3/4	1624	1190	1668	1191	1456	1153	1655	1224	1466	1221	1620	1212	1605	1251

Notes: All temperatures are in °F
surf = Surface temperatures
salt = Internal salt temperatures

Figure 2: Maximum and Minimum Cavity Temperatures

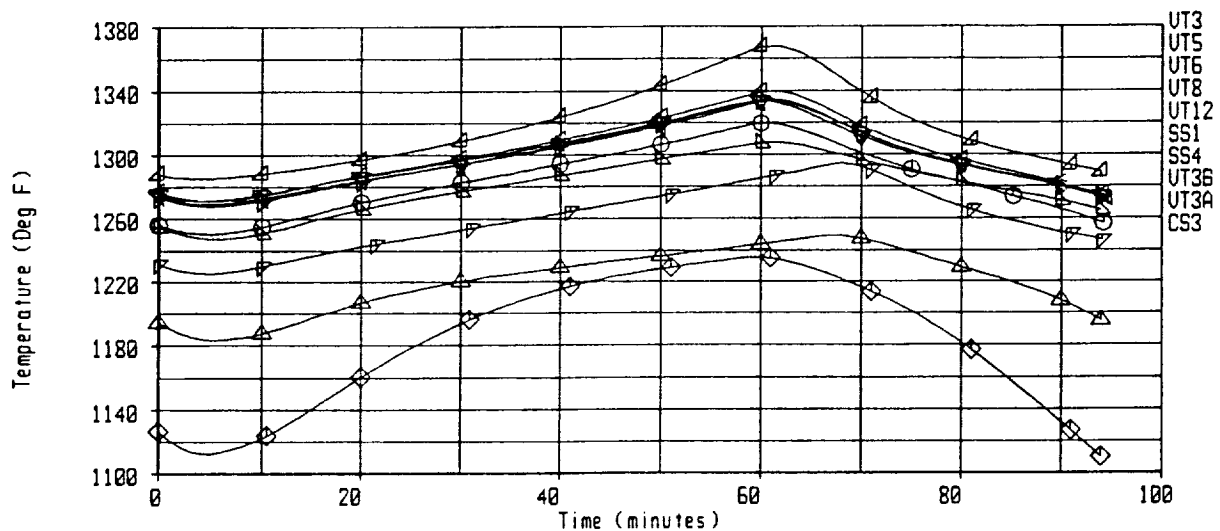


Figure 3: Comparison of Exiting Gas Temperatures



National Aeronautics and
Space Administration

Report Documentation Page

1. Report No. NASA TM-104486		2. Government Accession No.		3. Recipient's Catalog No.	
4. Title and Subtitle Full-Size Solar Dynamic Heat Receiver Thermal-Vacuum Tests				5. Report Date	
				6. Performing Organization Code	
7. Author(s) L.M. Sedgwick, K.J. Kaufmann, K.L. McLallin, and T.W. Kerslake				8. Performing Organization Report No. E-6332	
				10. Work Unit No. 474-52-10	
9. Performing Organization Name and Address National Aeronautics and Space Administration Lewis Research Center Cleveland, Ohio 44135-3191				11. Contract or Grant No.	
				13. Type of Report and Period Covered Technical Memorandum	
12. Sponsoring Agency Name and Address National Aeronautics and Space Administration Washington, D.C. 20546-0001				14. Sponsoring Agency Code	
15. Supplementary Notes Prepared for the 26th Intersociety Energy Conversion Engineering Conference cosponsored by ANS, SAE, ACS, AIAA, ASME, IEEE, and AIChE, Boston, Massachusetts, August 4-9, 1991. L.M. Sedgwick and K.J. Kaufmann, Boeing Aerospace and Electronics, Seattle, Washington; K.L. McLallin and T.W. Kerslake, NASA Lewis Research Center. Responsible person, T.W. Kerslake, (216) 433-5373.					
16. Abstract The first ever testing of a full-size, 102 kWt, solar dynamic heat receiver utilizing high-temperature thermal energy storage has been completed. The purpose of the test program was to quantify receiver thermodynamic performance, operating temperatures, and thermal response to changes in environmental and power module interface boundary conditions. The heat receiver was tested in a vacuum chamber with liquid nitrogen cold shrouds and an aperture cold plate to partially simulate a low-Earth-orbit environment. The cavity of the receiver was heated by an infrared quartz lamp heater with 30 independently controllable zones to allow axially and circumferentially varied flux distributions. A closed-Brayton cycle engine simulator conditioned a helium-xenon gas mixture to specific interface conditions to simulate the various operational modes of the solar dynamic power module on the Space Station Freedom. Inlet gas temperature, pressure, and flow rate were independently varied. A total of 58 simulated orbital cycles, each 94 minutes in duration, was completed during the test conduct period.					
17. Key Words (Suggested by Author(s)) Space stations; Solar dynamic power systems; Phase change materials; Heat storage; Brayton cycle; Solar collectors; Quartz lamps; Calcium fluorides; Lithium fluorides; Helium; Xenon; High temperature; Vacuum; Performance tests				18. Distribution Statement Unclassified - Unlimited Subject Category 20	
19. Security Classif. (of the report) Unclassified		20. Security Classif. (of this page) Unclassified		21. No. of pages 6	
				22. Price* A02	

